NANOSIGHT

...seeing is believing

NanoSight LM10-HSGT
Nanoparticle Analysis System
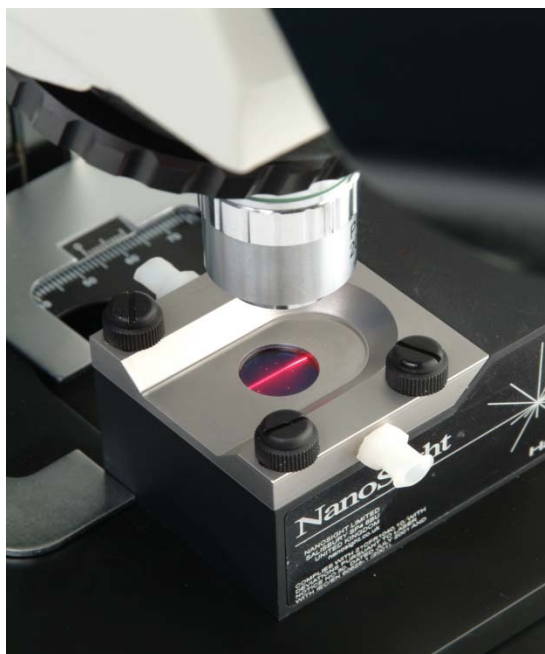
Viriditec™ Sample Test Report

Test carried out at BCG Solutions, LLC
September 5, 2012

Report prepared by: Sonja Capracotta, PhD.
Senior Applications Scientist
School of Public Health I
6611 Tower
1415 Washington Heights
Ann Arbor, MI 48109-2029
Tel: (815) 922-9215
email sonja.capracotta@nanosight.com

Tests performed by: Duncan Griffiths
Regional Manager
3027 Madeira Ave.
Costa Mesa, CA 92626

Tel: (714) 747-9955
Email duncan.griffiths@nanosight.com

NANOSIGHT

...seeing is believing

This report summarizes the measurement results for the samples provided during the demonstration.

Samples were analysed using the Nanosight LM10-HSGT nano-particle visualisation device, which employs the Nanoparticle Tracking Analysis technique as defined in ASTM 2834-12.

Short movie clips were captured and have been provided as *.wmv files for viewing by Windows Movie Player or QuickTime.

With this device the user can visualise individual particles down to approximately 10nm in diameter (material dependent) though it should be appreciated that the particles are not being <u>imaged</u> at this size scale (i.e. no structural or shape information is available), they are merely being visualised through the light they scatter.

Summary of Results:
A series of samples were presented for analysis during the demonstration. The concentration of particles for all samples was within the measurement range of the instrument and no dilution or other sample treatment was required. In this case the "particles" were nanobubbles, which scatter light and undergo Brownian motion in the same manner as a solid particle. See section below on background of the technique.

While the reported results are representative of what might be expected in normal use, further method development might provide improved analyses.

Sample	Mode Size (nm)	D10	D50	D90	Concentration (x 10^8 particles/ml)
Viriditec Sample 1	107	60	124	203	2.17
Viriditec Sample 2	154	45	120	179	1.44
Viriditec Sample 3	147	94	185	323	0.41
Viriditec Sample 4	93	46	162	248	0.38
Viriditec Sample 5	66	60	132	2.37	1.51

Discussion:
Samples 1, 2 and 5 were distinctly different in concentration from Samples 3 and 4. As explained, these were pulled from a different part of the process and were expected to show significant differences.

Referring to the overlay and individual results included below, all samples showed multi-modal distributions. With the relatively low concentrations of these samples and the limited measurement times used at the demonstration, the total number of particles counted were at the lower end of the optimum range. With increased analysis time and/or flowing the sample with a syringe pump, the number of particles measured will be increased, yielding a more robust measurement of each population. The individual peaks would be confirmed or may merge into a more continuous distribution.

All samples showed a similar range of sizes, with a lower size limit around 30nm and the tail of the larger sizes up to approximately 300nm.

In summary, the demonstration is intended to show how the system works and to give some example data in a relatively short time frame. The results and videos presented are a starting point to refine the methods and improve results.
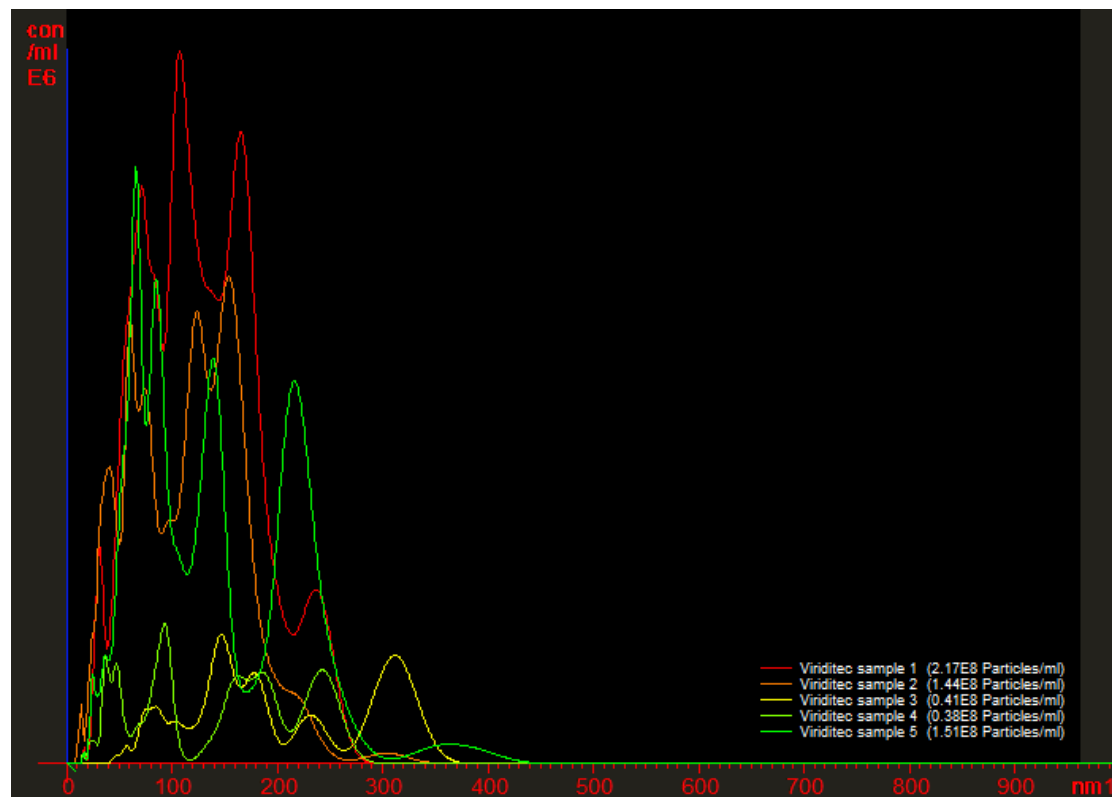
Figure 1: Overlay of all five samples showing range of sizes. Y-axis is concentration, showing samples 2 and 3 at significantly lower concentration.

Analysis Procedure

300µl of the sample was introduced into the NanoSight LM10-HSGT sample cell (532 nm, 50 mW laser) with a 1 ml disposable syringe and visualised using a conventional optical microscope (x20 long working distance objective 0.40NA) fitted with a scientific video camera (Hamamatsu CMOS). Images were collected directly to the hard drive as *.avi files with no further image processing.

Methodology

A finely focused laser beam is passed through a prism-edged optical flat, the refractive index of which is such that the beam refracts at the interface between the flat and a liquid layer placed above it. Due to the refraction, the beam compresses to a low profile, intense illumination region in which nanoparticles present in the liquid film can be easily visualised via a long-working distance, x20 magnification microscope objective fitted to an otherwise conventional microscope. Mounted on a C mount, a CMOS camera, operating at 30 frames per second, is used to capture a video field of view approximately 100µm x 80µm.
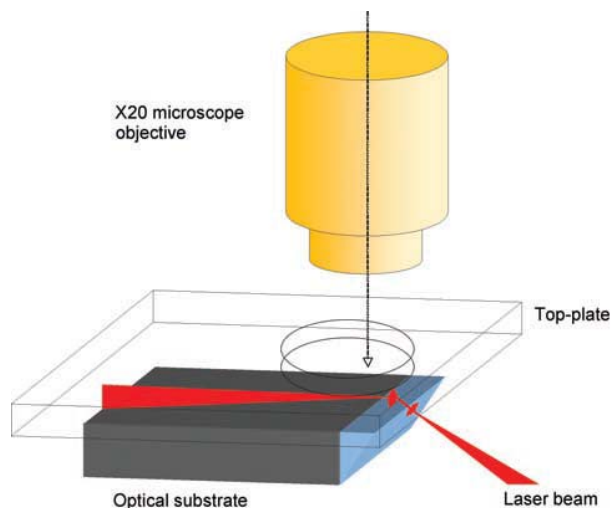
Figure 2: Schematic of LM10 optical system

Particles in the scattering volume are seen moving rapidly under Brownian motion. The NTA programme simultaneously identifies and tracks the centre of each particle on a frame-by-frame basis throughout the length of the video. Figure 3 shows an enlarged image of two such particles and the trajectory they have taken over several frames as tracked by the NTA image analysis programme.
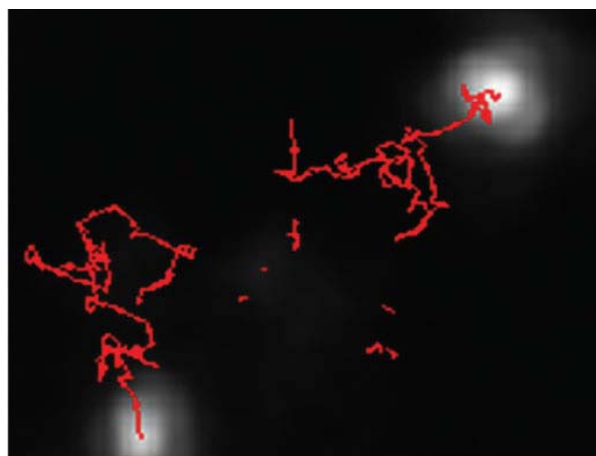
Figure 3: Particles being tracked by NTA software

The average distance each particle moves in x and y in the image is automatically calculated, from which the diffusion coefficient (Dt) and hence sphere-equivalent, hydrodynamic diameter (d) can be determined using the Stokes-Einstein equation:

$$Dt = \frac{K_B T}{3\pi\eta d}$$

where K_B is Boltzmann's constant, T is temperature and η is viscosity.

The range of particle sizes that can be analyzed by NTA depends on the particle type. The lower size limit is defined by the particle size and particle refractive index. For particles with very high refractive indices, such as colloidal gold, accurate determination of size can be achieved down to 10nm diameter. For lower refractive index particles, such as those of biological origin, the smallest detectable size might only be between 25 and 35nm. However, this minimum size limit allows the analysis of most types of virus. Upper

size limits are approached when the Brownian motion of a particle becomes too limited to track accurately, typically 1–2µm diameter.

To enable a sufficient number of particles to be analyzed within an acceptable time period (eg. <60 seconds) from which a statistically meaningful and reproducible particle size distribution profile can be obtained, samples should contain between 10^7 and 10^9 particles/ml, dilution of a sample often being required to achieve this concentration. The benefit of being able to measure two independent parameters simultaneously, such as particle-scattering intensity and particle diameter (from dynamic behavior) can prove valuable in resolving mixtures of different particle types (eg. distinguishing between inorganic and polymer particles of the same diameter). Similarly, small differences in particle size within a population can be resolved with far higher accuracy than would be achieved by other ensemble light-scattering techniques.

Reviewing Video Files

The image produced by the technique is a powerful aide when analysing a sample and a cursory glance can help make sense of unexpected results. The scattering intensity of a particle is dependent upon its size (with larger particles scattering more light) and also its refractive index. The Brownian motion however, is dependent only upon the particle size, solvent viscosity and temperature (and is absolutely independent of particle density) and therefore provides an absolute measure of particle size, with smaller particles having a more exaggerated motion.

A still from the video may be misleading in that the bright particles may be associated with larger particles when in fact the intensity of the particle may be associated with the refractive index of the particle. The video clip however can be used to qualitatively asses the size of the particle both by the intensity and its Brownian motion (with the Brownian motion only being used to size the particle).

As the image produced is not a direct image of the particles themselves merely the light which they scatter it is difficult to tell if the larger particles within the samples are aggregates or if they are naturally present as a result of formulation techniques.
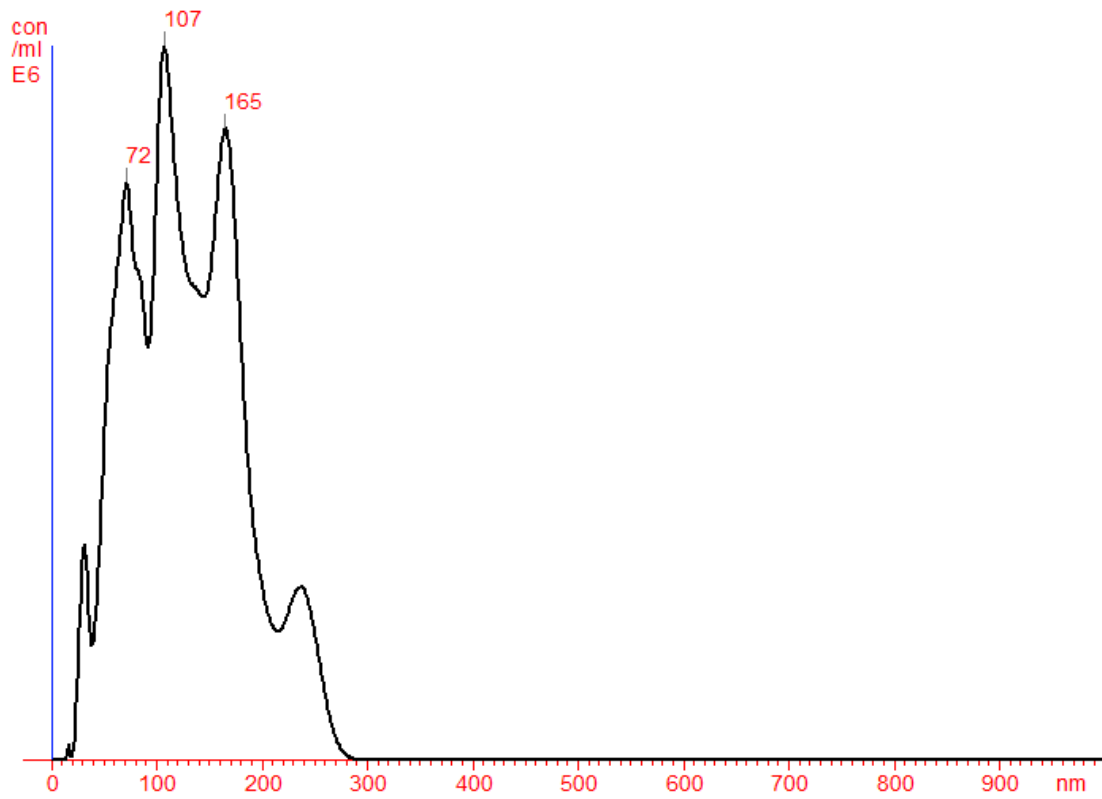
Figure 4: Viriditec™ Sample 1
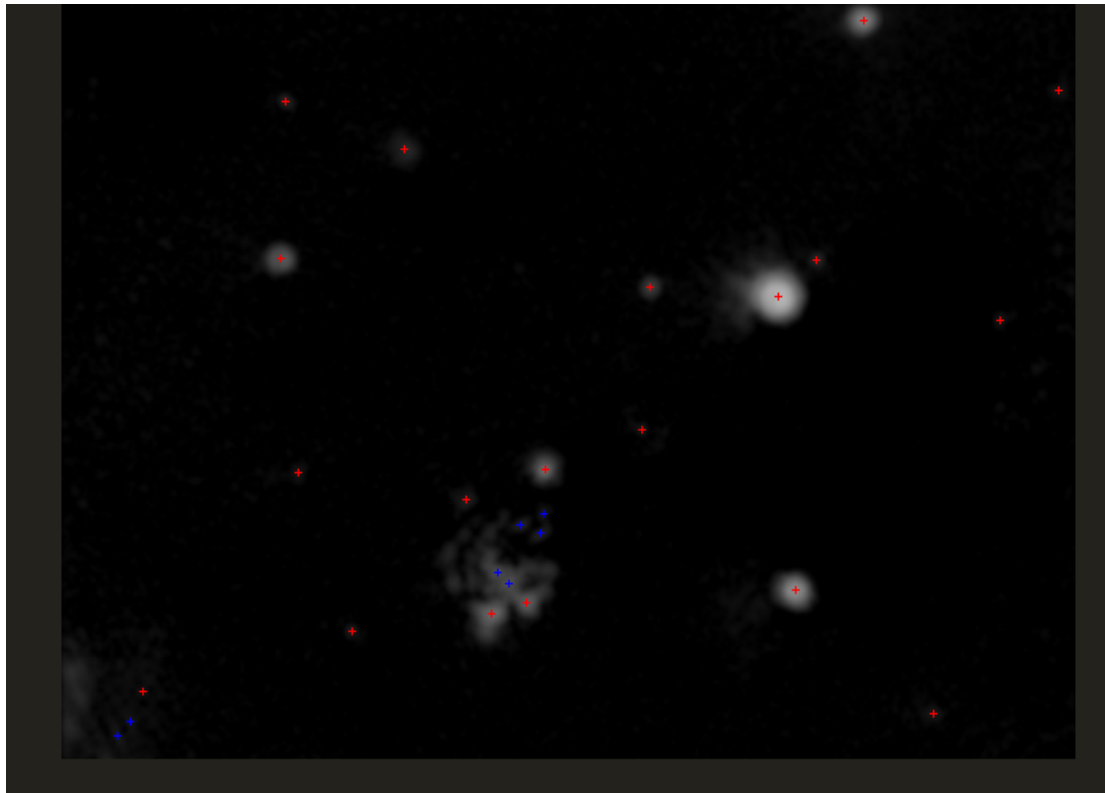
Figure 5: Still from video of Sample 1.
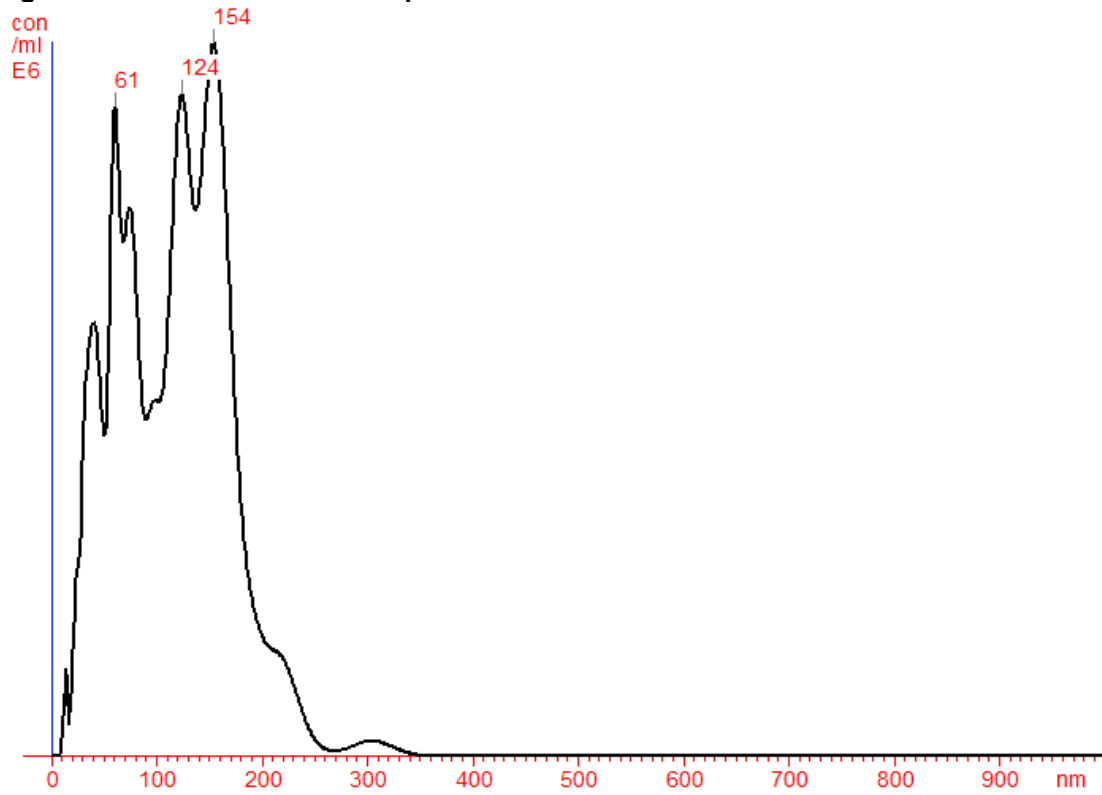
Figure 6: Viriditec™ Sample 2
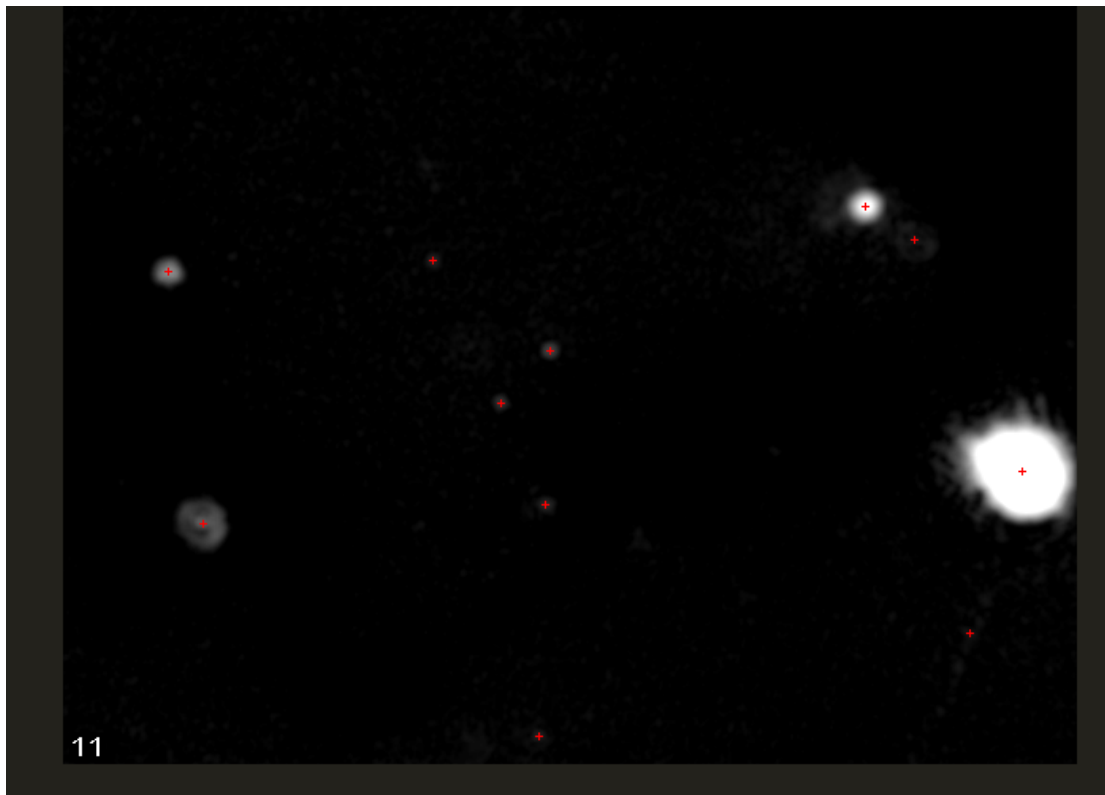
Figure 7: Still from video of Sample 2.
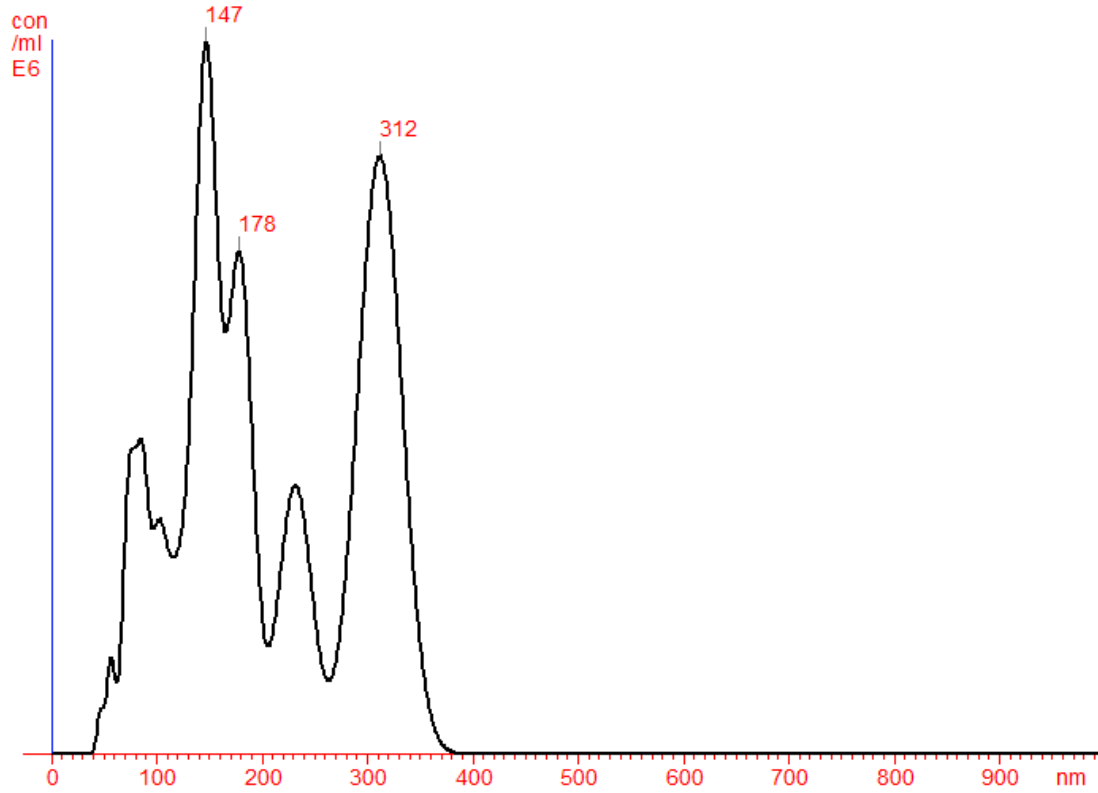
Figure 8: Viriditec™ Sample 3
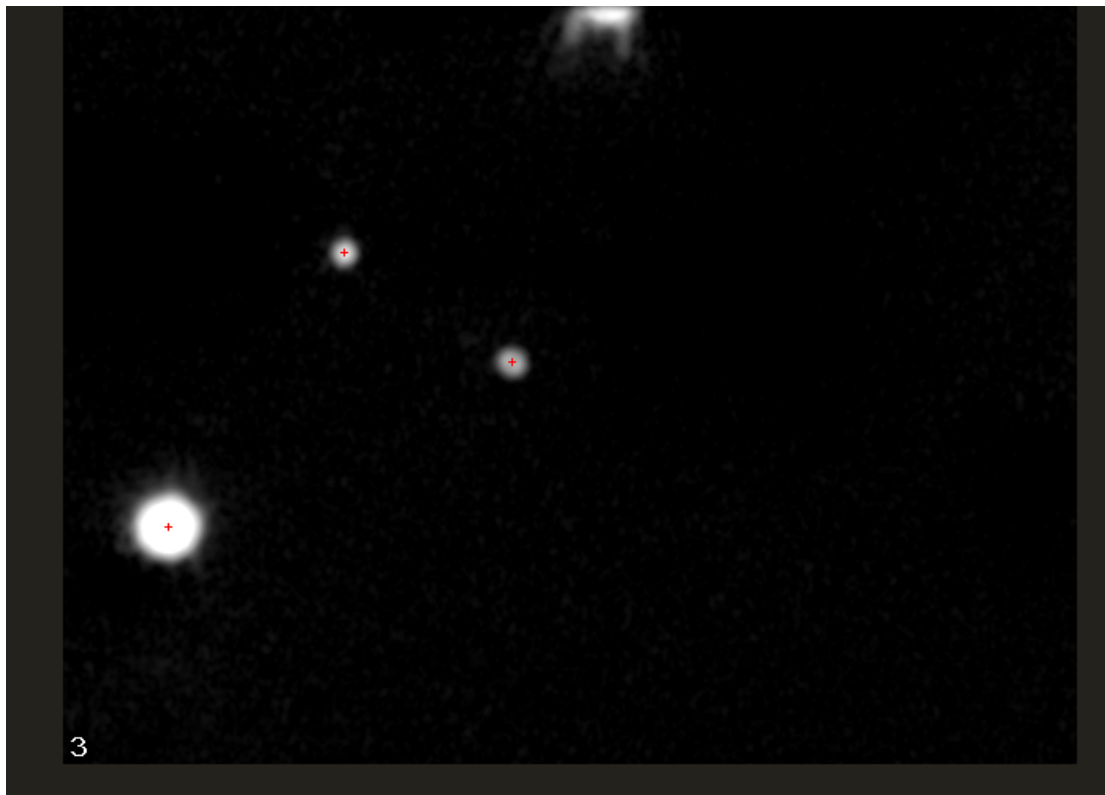
Figure 9: Still from video of Sample 3.
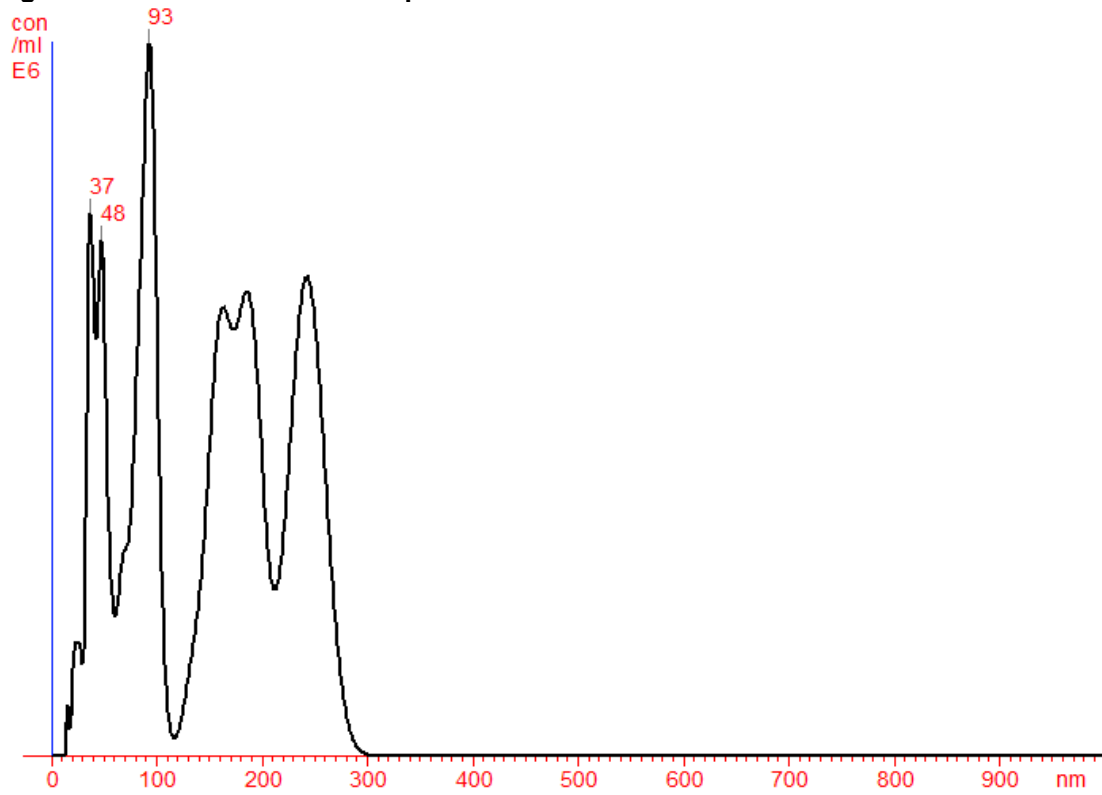
Figure 10: Viriditec™ Sample 4
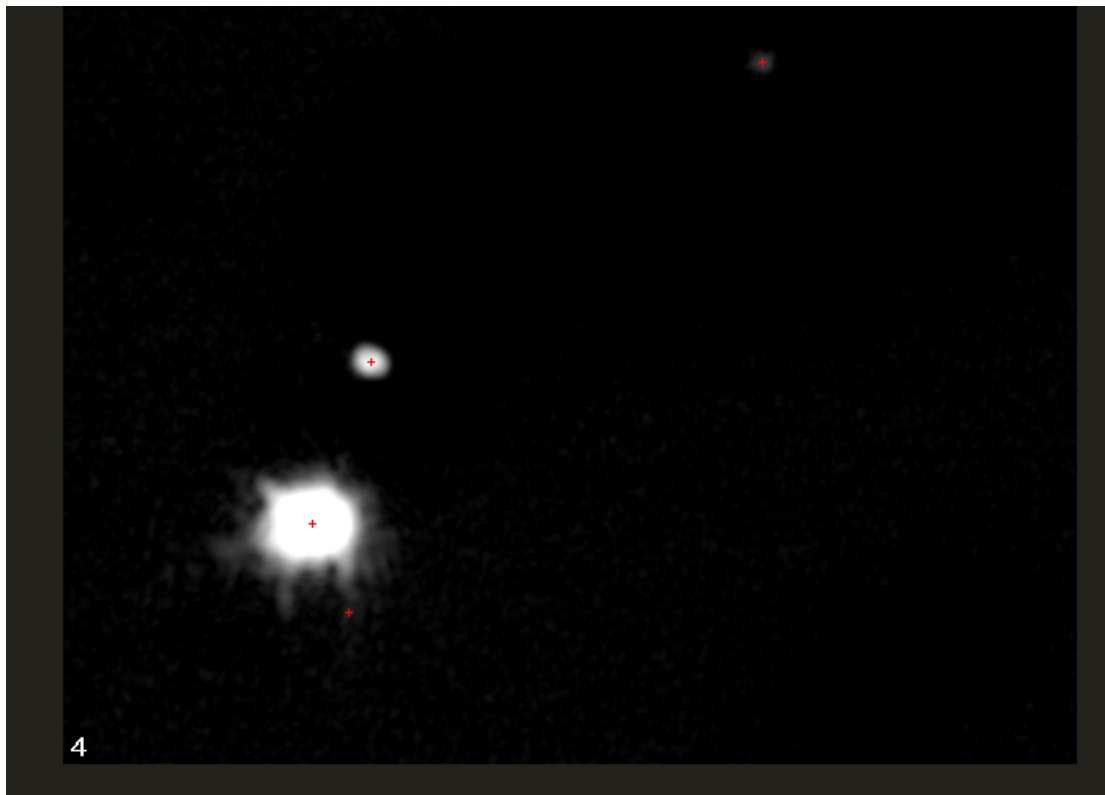
Figure 11: Still from video of Sample 4.
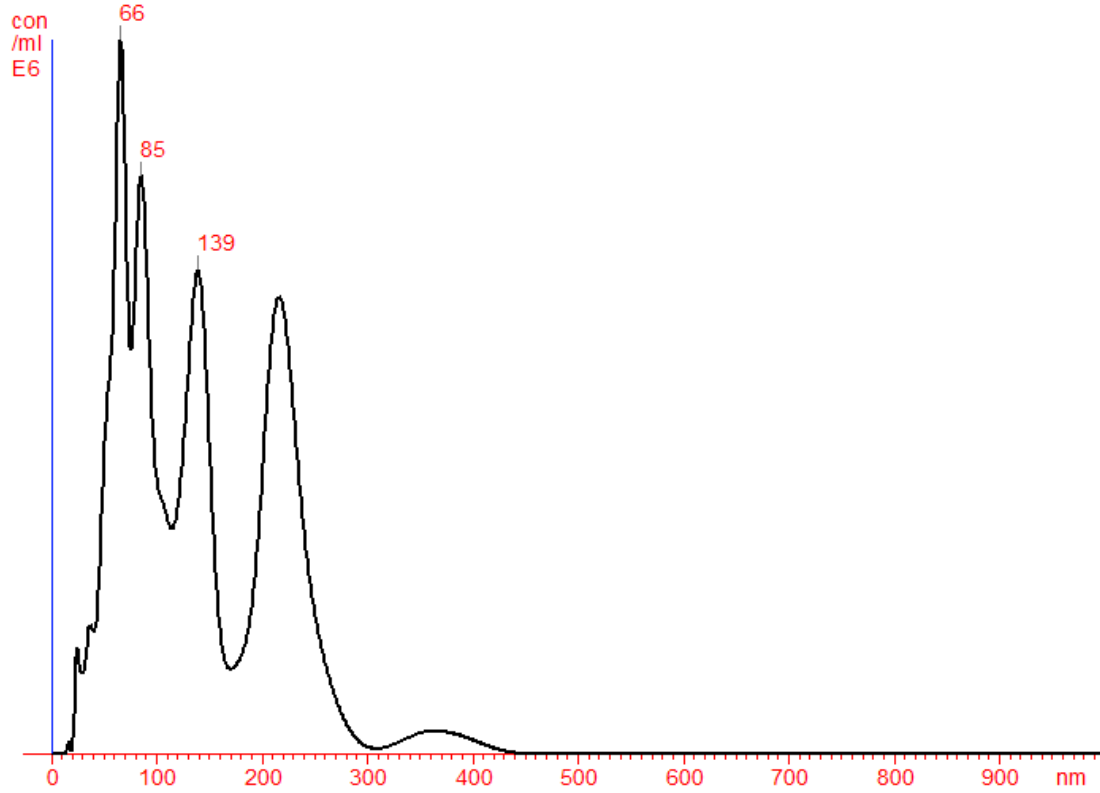
Figure 12: Viriditec™ Sample 5
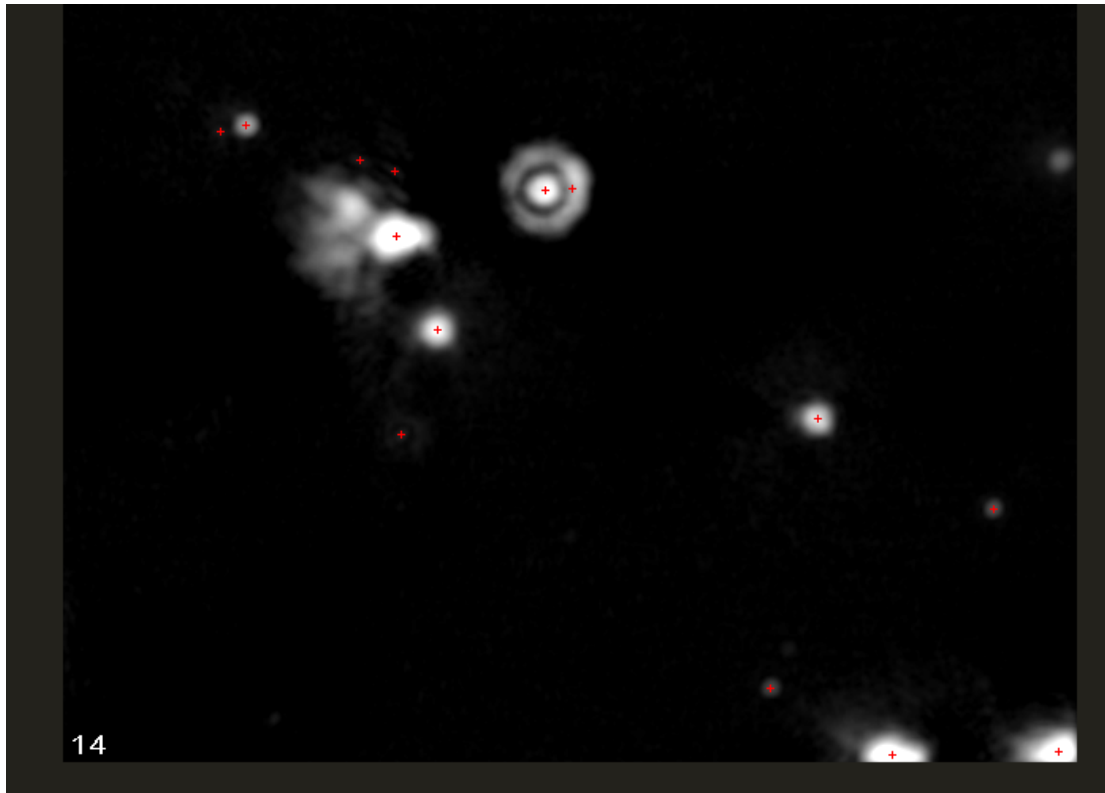
Figure 13: Still from video of Sample 5.

Nanobubbles – a New Class of Structure Ready for Exploitation?

Background

Despite initial scepticism, acceptance of the existence and special properties of nanobubbles is now growing and their formation and characteristics are now becoming the subject of an increasing amount of study, especially in Japan.

Due to the supposed very high pressure within bubbles of such small size and radius of curvature, and thus high surface tension, conventional calculations show that the gas should be 'pressed out' of the nanobubbles within microseconds. However, it is now clear that under the right conditions such bubbles can both form freely and remain stable for extended periods of time, sometimes for many months. Explanations as to just why such structures are so stable are focussing on the role of counter-ions forming layers at the nanobubbles surface, explaining claims that they apparently form only in the presence of salts.

Kaneo Chiba and Masayoshi Takahashi of Japan's famous AIST research centre have shown that in the presence of electrolytes and with the correct physical stimulus, stable nanobubbles can be formed from conventional microbubbles. The latter tend to coalesce to large buoyant bubbles which either float away or collapse under intense surface tension-derived pressure to the point that they vanish, as predicted by theory. However, the addition of salt (electrolytes) is thought to cause the formation of a counter-ion screen around the nanobubbles which effectively blocks the ability of gases within them to diffuse out.

Furthermore, Prof. William Drucker of the University of Melbourne has also used infra-red spectroscopy to show that the pressure of gas within such nanobubbles is not significantly higher than atmospheric pressure, perhaps explaining their stability and resistance to collapse.
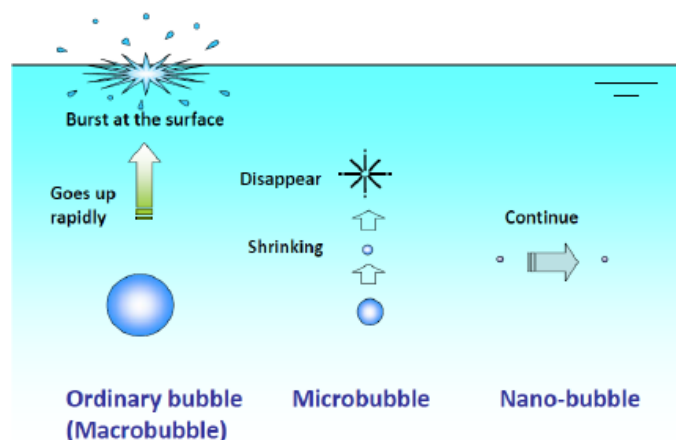
Figure 1. The formation of nanobubbles.

Measuring Nanobubbles

In an earlier study, Kikuchi et al (2001) showed that the formation of hydrogen nanobubbles was related to the influence of electrolysis conditions on the hydrogen content and the diameter distribution of hydrogen nanobubbles. In this study, Dynamic Light Scattering (DLS) was used to analyse the nanobubbles. However, in a recent study of the formation and characterisation of nanobubbles in water by a major pharmaceutical company in Japan, the concentration of nanobubbles in a mechanically formed suspension was found to be very low (<10^7/ml),

a concentration which would be too low for meaningful analysis by DLS. Of course, analysis by Electron Microscopy was not possible because of the vacuum required for EM studies.

NanoSight was shown to be ideally suited to such analyses. In a blind experiment in which three samples of nanobubble suspensions containing high, low and zero numbers of nanobubbles were tested in duplicate, NanoSight results were found to match exactly those predicted. The graph shows the results in which sample A (series 1 and 6) contained a high concentration of nanobubbles, sample B (series 3 and 5) contained a low concentration of nanobubbles and sample C (Series 2 and 4) were control blanks. It should be noted that NanoSight measures concentration of nanobubbles per unit volume as well as size and size distribution.
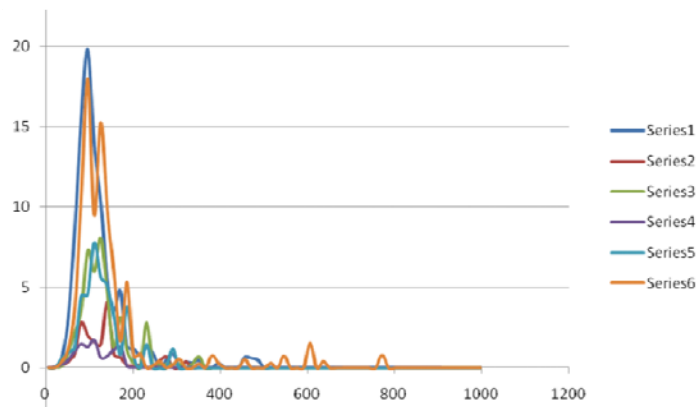
Figure 2. NanoSight results

More recently, Ichiro Otsuka (2008) of Ohu University, Japan has studied the possible role of nanobubbles in ultra-high diluted samples of active agents in which the phenomenon of succussion is considered relevant. He used NanoSight technology to examine nanobubble formation and concentration in more detail than was possible using an electrozone (Coulter) method or conventional DLS techniques.

Applications

There exists a wide range of proposed nanobubble applications and interest in their usage is growing rapidly. When formed from ozone and electrolyte stabilised, disinfection and sterilisation is possible for many months with great potential in the preservation of foodstuffs and in medical applications as an attractive alternative to chlorine based methodologies.

Oxygen nanobubbles have been implicated in the prevention of arteriosclerosis by the inhibition of mRNA expression induced by cytokine stimulation in rat aorta cell lines.

When formed in liquids in capillaries, nanobubbles have been shown to greatly improve liquid flow characteristics. They have also been proposed as contrast agents in scanning techniques as well as cleaning agents in silicon manufacturing processes.

Finally, a new field of drug delivery applications is being actively researched in which nanobubbles play an active part though details of this highly secretive field are hard to come by. However, reported in Reuters, Natalya Rapoport of the University of Utah's Department of Bioengineering is using nanobubbles with the chemotherapy drug doxorubicin to seek out and congregate at cancer tumors when injected into the bloodstream. "These nanobubbles don't penetrate normal blood vessels but they do penetrate blood vessels in the tumor," said Rapoport, whose study appears in the Journal of the National Cancer Institute. Once in the tumor, the nanobubbles combine to form larger microbubbles which can be seen on an ultrasound. "When these bubbles accumulate, I give strong ultrasound radiation to the tumor to blow them up," she said in a telephone interview. "The drug then gets out of these bubbles locally at the tumor site."

In Conclusion

NanoSight has proved uniquely capable of visualising, sizing and counting nanobubbles in liquids. The concentration ranges encountered in this application frequently appear ideal for analysis by NTA.

Kenji Kikuchi, Hiroko Takeda, Beatrice Rabolt, Takuji Okaya, Zempachi Ogumi, Yasuhiro Saihara and Hiroyuki Noguchi (2001) Hydrogen particles and supersaturation in alkaline water from an alkali–ion–water electrolyzer, Journal of Electroanalytical Chemistry, p1–6

Ichiro Otsuka (2008) Effect of 1:2 aqueous dilution on O2 nanobbubles in a 0.1 M Na2CO3 solution, Proc The 59th Annual Meeting of the International Society of Electrochemistry, September 7 to 12, 2008, Seville, Spain; s10-P-062, p139